Detection and Characterization of the Lignin Peroxidase Compound II−Veratryl Alcohol Cation Radical Complex†

Aditya Khindaria, Guojun Nie, and Steven D. Aust*

Biotechnology Center, Utah State University, Logan, Utah 84322-4705

Received June 30, 1997; Revised Manuscript Received September 4, 1997⊗

ABSTRACT: Lignin peroxidases (LiP) from the white-rot fungus *Phanerochaete chrysosporium* oxidize veratryl alcohol (VA) by two electrons to veratryl aldehyde, although the VA cation radical ($VA^{\bullet+}$) is an intermediate [Khindaria, A., et al. (1995) *Biochemistry 34*, 6020−6025]. It was speculated, on the basis of kinetic evidence, that $VA^{\bullet+}$ can form a catalytic complex with LiP compound II. We have used low-temperature EPR to provide direct evidence for the formation of the complex. The EPR spectrum of $VA^{\bullet+}$ obtained at 4 K was explained by a model for coupling between the oxoferryl moiety of the heme ($S = 1$) and $VA^{\bullet+}$ ($S = 1/2$) similar to the model proposed for an oxyferryl and a porphyrin π cation radical of horseradish peroxidase. The coupling constant suggested that $VA^{\bullet+}$ was equally ferro- and antiferromagnetically coupled to the oxoferryl moiety. The spectrum was simulated with $\mathbf{g}_\perp$ only marginally greater than $\mathbf{g}_\parallel$. This was surprising since the only other known organic radical coupled to the heme iron in a peroxidase is the tryptophan cation radical in cytochrome c peroxidase which exhibits a **g** tensor with $\mathbf{g}_\parallel$ greater than $\mathbf{g}_\perp$. Spin concentration analysis suggested that the 1 mol of $VA^{\bullet+}$ was coupled to the oxoferryl moiety per mole of enzyme. The $VA^{\bullet+}$ signal decayed with a first-order decay constant of 1.76 s^{-1}, in close agreement with the earlier published decay constant of 1.85 s^{-1} from room-temperature EPR studies. The exchange coupling between $VA^{\bullet+}$ and the oxoferryl moiety strongly advocates calling this species ($VA^{\bullet+}$ and LiP compound II) a catalytic complex.

Lignin peroxidases (LiP), a group of heme-containing extracellular enzymes, are important components of the lignin degrading system of the white-rot fungus *Phanerochaete chrysosporium*. LiP catalyzes nonspecific one-electron oxidations of lignin, a three-dimensional stereoirregular structural polymer made up of phenylpropanoid units (Sarkanen & Ludvig, 1971). The resultant cation radicals of lignin fragment through $C_\alpha-C_\beta$ bond cleavage (Tien & Kirk, 1983). Various studies support such a direct role of LiP in lignin degradation (Hammel & Moen, 1991; Tien & Kirk, 1983, 1984). However, this mechanism has been questioned due to the unlikely direct interaction between lignin and the heme prosthetic group of the enzyme (Poulos et al., 1993). The three-dimensional X-ray diffraction structure of LiP shows that the heme in LiP is buried inside the protein with only a small opening connecting the active site with the outside of the protein (Poulos et al., 1993). Small molecules can possibly diffuse in and out of this opening, but there is no evidence that a bulky polymer like lignin can access the active site through this opening. Therefore, the question then arises, how is lignin oxidized by LiP?

One of the most promising hypotheses, with abundant supporting data, is that small molecule mediators form an electron shuttle resulting in lignin oxidation. In this case, a small molecule mediator would be oxidized by LiP to a cation radical which could then oxidize lignin, itself being reduced to the parent compound. One such mediator is veratryl alcohol [3,4-(dimethoxy)benzylalcohol; VA] (Goodwin et al., 1995; Chung & Aust, 1995), which is a secondary metabolite produced by *P. chrysosporium* (Lundquist & Kirk, 1978). It is a substrate for LiP and is synthesized and secreted extracellularly by *P. chrysosporium* under lignolytic conditions (Shimada et al., 1981). It is oxidized by LiP to a cation radical ($VA^{\bullet+}$) (Harvey et al., 1986; Gilardi et al., 1990; Khindaria et al., 1995a) and then to veratryl aldehyde (Khindaria et al., 1995a). The first electron-transfer step is easy to understand. However, the mechanism of second electron oxidation of $VA^{\bullet+}$ to veratryl aldehyde is still unclear. Kinetic data suggests that $VA^{\bullet+}$ exists as a complex with LiP compound II (LiPII) and is not released into the bulk solution (Khindaria et al., 1995b). It is also known that the complex of $VA^{\bullet+}$ and LiPII is catalytically active and reacts with an additional molecule of VA to form veratryl aldehyde. Indirect evidence is accumulating for the formation of this complex. However, direct electron paramagnetic resonance (EPR) detection and characterization of this complex has not been reported.

Magnetic and spectral characterization of this complex would shed more light on the role of VA as a redox mediator and allow us to better understand the mechanism of veratryl aldehyde formation. We have employed liquid helium temperature EPR for detection of this complex and have demonstrated magnetic and electronic interactions between LiPII and $VA^{\bullet+}$. We also demonstrate that spin−spin and orbital interactions modulate the properties of $VA^{\bullet+}$.

MATERIALS AND METHODS

Materials. Hydrogen peroxide was purchased from Sigma Chemical Co. Veratryl alcohol, sodium succinate, and succinic acid were purchased from Mallinckrodt. All chemicals were reagent grade and used without further

† This work was supported in part by Stockhausen GmbH and Co. KG., P.O. Box 570, D-47705/Krefeld, Germany.

* To whom correspondence should be addressed.

⊗ Abstract published in *Advance ACS Abstracts,* November 1, 1997.

S0006-2960(97)01573-0 CCC: $14.00

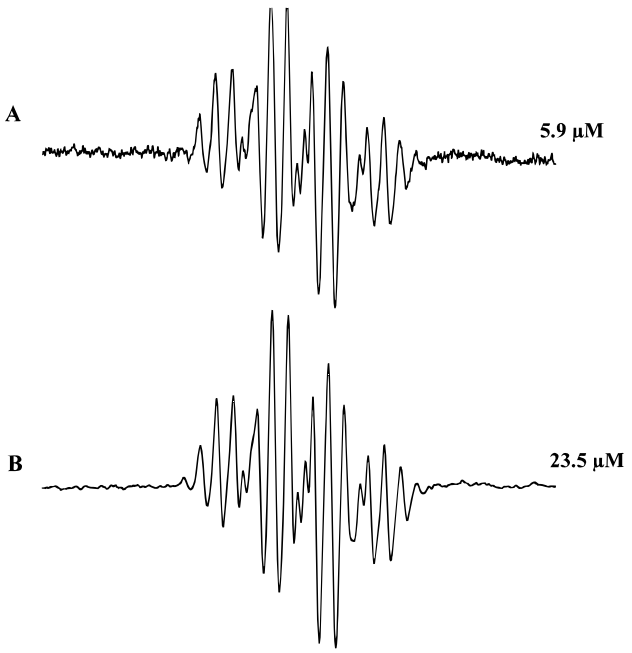

FIGURE 1: Room temperature EPR spectra of $VA^{\bullet+}$. Spectrum A was recorded in a flow system with 25 μM LiP, 2 mM VA, and 500 μM H_2O_2. Spectrum B was recorded under the same conditions as A except that 10% HNO_3 was added just before acquisition. The numbers on the right are the concentrations of $VA^{\bullet+}$ as measured by double integration of the EPR spectrum with Tempol as a reference. The EPR spectrometer was operated at 9.7 GHz and 50 KHz modulation frequency.

purification except VA, which was vacuum distilled to rid it of a trace phenol contaminant (Tien et al., 1986). All buffers and solutions were prepared using purified water (Barnstead NANOpure II system; specific resistance 18.0 $M\Omega$ cm^{-1}). Pure lignin peroxidase isozyme H2 (pI = 4.4) was used throughout the study and was purified as described previously (Tuisel et al., 1990).

EPR Measurements. All EPR measurements were performed on a Bruker ESP300 spectrometer equipped with a Oxford ESR 10 helium flow cryostat and DTC-2 temperature controller. Instrument settings are given in figure legends. EPR power saturation data were collected by measuring the EPR absorption derivative signal intensity as a function of microwave power at different temperatures. The saturation data were fit to the expression

$$S/P_{1/2} \propto 1/(1 + P/P_{1/2})^{1/2} \quad (1)$$

where S is the derivative signal intensity, P is the microwave power, and $P_{1/2}$ is the half saturation power. A nonlinear least-squares fit to the above equation yielded a $P_{1/2}$ value for each particular temperature.

RESULTS AND DISCUSSION

The EPR spectra of $VA^{\bullet+}$ under normal turnover and acid-quenched conditions are shown in Figure 1. Spectrum A decayed with a first-order decay constant of 1.8 s^{-1} while spectrum B decayed with a decay constant of 9×10^2 s^{-1}. These are essentially identical to those published earlier (Khindaria et al., 1996) where we had suggested that even though the $VA^{\bullet+}$ spectra under two conditions are similar the species may be different. During turnover, $VA^{\bullet+}$ forms a complex with LiPII and exists in two forms, EPR active and EPR silent. By definition, only the EPR-active form (ca. 20% of LiP concentration) was detected during turnover. Upon acid quenching though, the enzyme was denatured and the EPR-silent form was detected. The concentration of $VA^{\bullet+}$ under acid quenched conditions reached approximately 95% of LiP concentration. Coupling of $VA^{\bullet+}$ with the heme iron may result in fast relaxation (τ) and broadening of the $VA^{\bullet+}$ EPR signal at room temperature. Therefore, it was important to quantitate the contribution of this coupling to τ, the spin−spin relaxation time.

It has been established that τ often is a measure of the interaction between spins. In this case, if $\tau = \infty$, the spins are completely isolated from each other, whereas $\tau = 0$ implies very strong coupling. The species can interact via magnetic dipolar coupling. Note that mutual spin flips of species cause no change in energy of spin but do affect the spin−spin relaxation lifetime (τ) of each species. Spin relaxation times are inversely dependent on temperature. This interaction between the species can be analyzed at very low temperature because the spin−spin coupling can be increased by lowering temperature. Therefore, we employed liquid helium temperatures to study the possible magnetic spin diffusion through the lattice that could have caused equilibration throughout the system of equivalent spins.

Reaction mixtures containing LiP and VA were frozen in a slurry of liquid N_2 and hexane within 500 ms of initiation of the reaction with H_2O_2. The EPR spectrum obtained at 4 K from the complete reaction mixture is shown in Figure 2. The EPR signal exhibited a broad, axially symmetric signal at $\mathbf{g} = 2.0034$. This signal was not observed when VA or H_2O_2 were left out of the reaction mixture (data not shown). The line width of the signal was 22.5 G. These parameters were in striking contrast to the EPR signal due to LiP compound I (LiPI), $\mathbf{g} \approx 1.96$ and line width $\approx$ 12 G (Khindaria & Aust, 1996). Therefore, this signal was not due to LiPI and was tentatively assigned to $VA^{\bullet+}$. We tried using various models, including those proposed for certain protein radicals, to simulate the EPR spectrum of $VA^{\bullet+}$. None of these models that sought to explain the EPR spectrum of $VA^{\bullet+}$ based on isolated spin could explain the spectrum. We then employed a model where the oxoferryl moiety ($S = 1$) was assumed to be spin coupled with the cation radical ($S' = 1/2$) according to a model proposed by Schultz et al. (1979). The Hamiltonian to explain the EPR spectrum can be written as $H = JSS'$, where J is the coupling constant between the cation radical and the oxoferryl moiety. This, in combination with a positive zero field splitting at the $[Fe = 0]^{2+}$ moiety (splitting parameter, D), causes 6 energy levels $[(2S + 1)(2S' + 1) = (3)(2)]$ of the oxiferryl−$VA^{\bullet+}$ system to form three Kramer's doublets. The lowest doublet is well separated in energy from the other two and gives rise to the observed EPR spectrum. The observed spectrum can be represented in terms of the effective spin ($s_{eff} = 1/2$). Effective $\mathbf{g}$ values, ($\mathbf{g}_{\perp eff}$ and $\mathbf{g}_{\parallel eff}$) are determined by the ratio J/D (Schultz et al., 1979; Rutter et al., 1984). To a first approximation, $\mathbf{g}_{\perp eff} \approx \mathbf{g}_e$ and $\mathbf{g}_{\perp eff} \approx \mathbf{g}_e - 2\mathbf{g}_{\perp}^{Fe} J/D$, where $\mathbf{g}_{\perp}^{Fe}$ describes the isolated $(Fe = 0)^{2+}$ oxoferryl moiety and its value is 2.25 for the oxoferryl heme (Hoffman et al., 1981) and J/D is the ratio of exchange coupling to the zero field splitting parameter. As D is expected to be greater than zero for the oxoferryl heme center, a value of $\mathbf{g}_{\perp eff}$ that is greater than $\mathbf{g}_{\parallel eff}$ results from ferromagnetic coupling (J

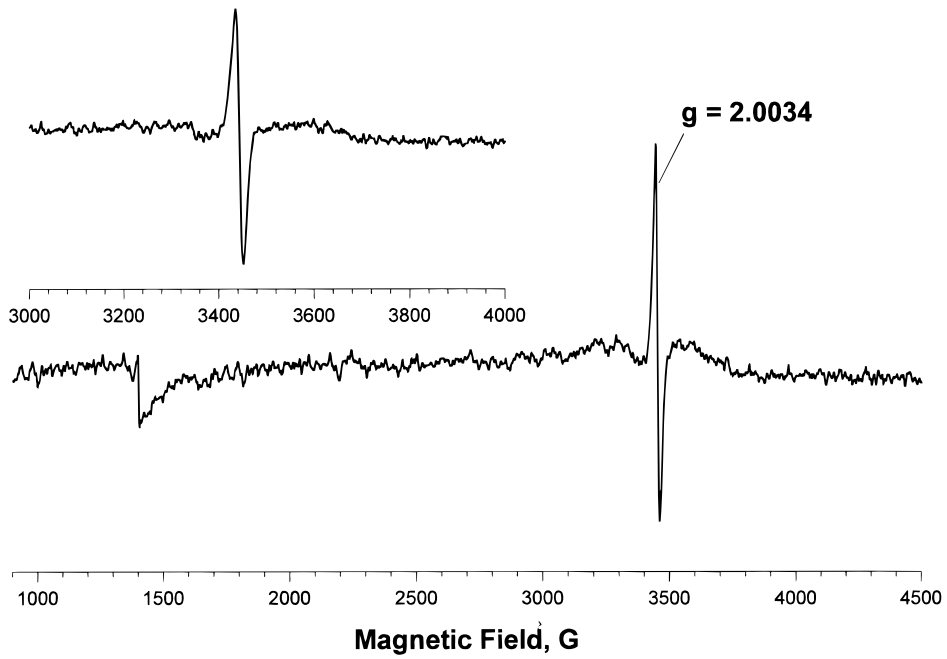

FIGURE 2: EPR spectrum of $VA^{\bullet+}$ at 4 K. A reaction mixture containing 250 μM LiP, 10 mM VA, and 5 mM H_2O_2 was frozen in a slurry of liquid N_2 and hexane within 500 ms of the initiation of the reaction with H_2O_2. Spectrometer settings were microwave frequency, 9.64 GHz; microwave power, 1 μW (42 dB); modulation amplitude, 5 G; modulation frequency, 100 kHz; time constant, 163 ms; scan time, 163.85 s, gain, 1×10^4. Inset shows the expanded $g \approx 2$ EPR signal.

< 0). Conversely, $\mathbf{g}_{\perp\text{eff}}$ would be less than $\mathbf{g}_{\|\text{eff}}$ for antiferromagnetic coupling ($J > 0$). For $VA^{\bullet+}$ and the oxoferryl system $|J|/D \approx 0.06$ and within reasonable error may be assumed to be 0.

Interestingly, exchange couplings characterized by ratios in this range cause a negligible (<3%) change in the hyperfine couplings to the protons on the radical, here the protons on the $VA^{\bullet+}$. These data are in agreement with our earlier room-temperature EPR studies on $VA^{\bullet+}$ (Khindaria et al., 1995a,b). We had assumed, based on kinetic evidence, that the EPR-silent form, spin coupled to the oxoferryl moiety, and the EPR-active form were in dynamic equilibrium (Khindaria et al., 1995b). This had prompted reviewers to suggest that the signal for the EPR-active form should be affected by the dynamic exchange between the two states. However, this was not observed, and we had no explanation for this phenomenon. Now, with spin-coupling data, it is evident why the line shape and the proton hyperfine splittings were not affected and the EPR signal of $VA^{\bullet+}$ during turnover and under acid quenched conditions were similar if not identical (Khindaria et al., 1995a,b; Figure 1).

Further evidence that the oxoferryl moiety affects the EPR signal of $VA^{\bullet+}$ comes from power saturation data. These data can also be used to determine the temperature dependence of the spin-lattice relaxation time. According to our model, the $VA^{\bullet+}$ is spin coupled to the oxoferryl moiety which has a large zero-field splitting parameter, D. The resulting system consists of three Kramer's doublets, the lowest of which is responsible for the observed EPR spectrum. The temperature dependence of the spin-lattice relaxation rate was measured by the method of progressive saturation and a summary of the results is shown in Figure 3. A plot of ln $P_{1/2}$ as a function of $1/T$ yielded a straight line with the slope equal to excited state energy, $\Delta = 23$ K. For weak coupling, $|J| << D \approx 20$ K, the ground doublet which gives rise to the EPR signal, is separated from the excited states by an energy $\Delta \approx D$. Since phonon-induced

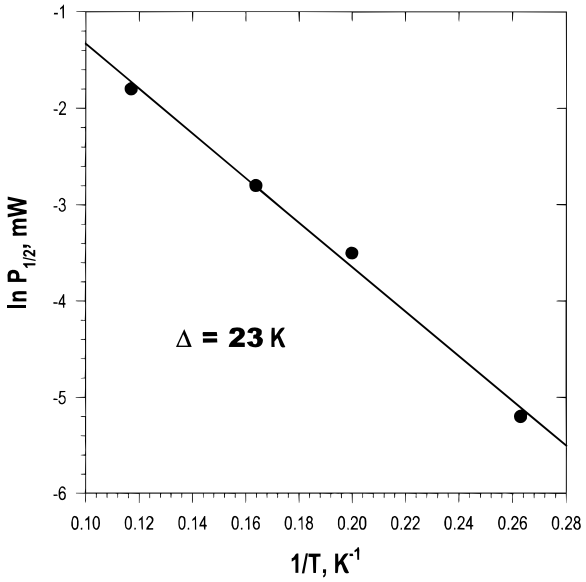

FIGURE 3: Half-saturation power of the $g \approx 2.0$ EPR signal of $VA^{\bullet+}$ as a function of temperature. The half-saturation values $P_{1/2}$ were calculated as described in the methods section. All parameters were the same as those for Figure 2 except that modulation frequency of 1 KHz was used. The solid line is a fit of the logarithm of $P_{1/2}$ according to $S/P_{1/2} \propto 1/1(1 + P/P_{1/2})^{1/2}$. The slope of the plot gives the excited state energy, $\Delta = 23$ K.

transitions within a doublet are forbidden in first order, spin relaxation is dominated by Orbach processes via excited states. Therefore, from these data the zero-field splitting can be predicted, within reasonable error, to be 23 cm^{-1}.

At this point, it was evident that $VA^{\bullet+}$ formed during LiP turnover was spin coupled to the heme iron. Earlier, we had demonstrated that (1) $VA^{\bullet+}$ is not released into bulk solution, (2) it is stabilized by LiP (Khindaria et al., 1995b, 1996), and (3) if LiP is denatured, then the decay rate of $VA^{\bullet+}$ increases 700-fold (Khindaria et al., 1996). We also demonstrated that $VA^{\bullet+}$ exists in two forms, EPR active and

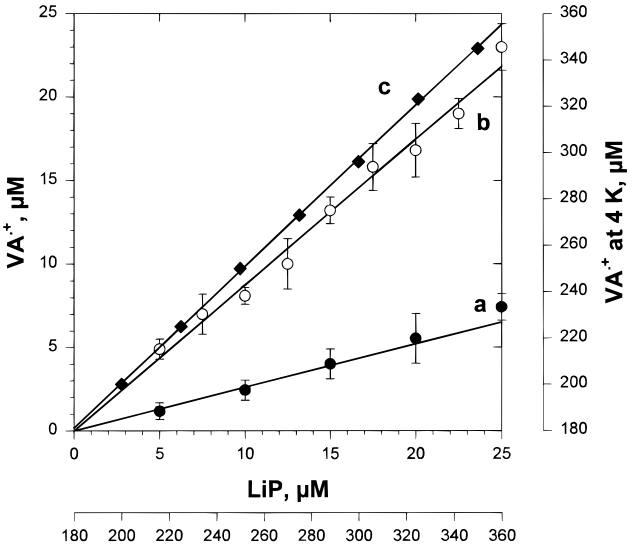

FIGURE 4: Effect of LiP concentration on the concentration of $VA^{\bullet+}$ under different conditions. Plot a (●) represents the concentration of $VA^{\bullet+}$ at room temperature during normal turnover. Plot b (○) represents the concentration of $VA^{\bullet+}$ at room temperature but under acid quenched conditions. The reaction conditions for plots a and b were the same as those described in Figure 1 for spectrum A and B, respectively. Plot c (◆) represents the concentration of $VA^{\bullet+}$ (formed by oxidation with LiP at room temperature) at 4 K. The reaction conditions were the same as described for Figure 2 except that LiP concentrations were varied as indicated. All concentrations were determined by double integration of the EPR spectrum and using Tempol as a standard. The data points are averages of three acquisitions and the error bars represent the standard deviation.

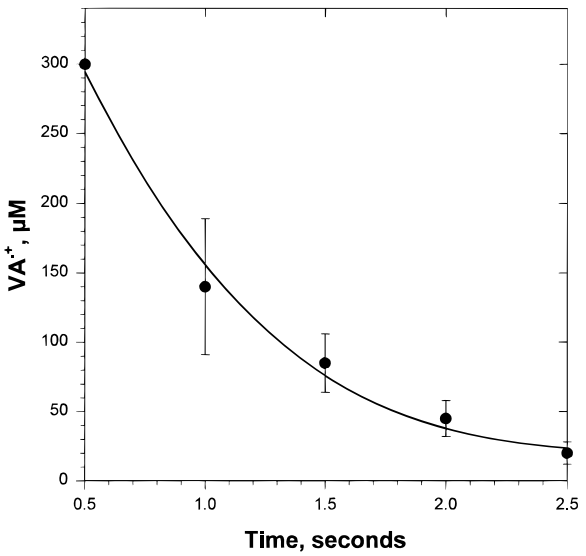

FIGURE 5: The decay of $g \approx 2.0$ EPR signal $VA^{\bullet+}$. Reaction mixtures containing equimolar concentration (330 μM) of LiP, VA and H_2O_2 were frozen in a slurry of liquid N_2 and hexane at various times after the reaction was initiated at room temperature. Spectrometer settings were the same as described in Figure 2.

EPR silent, that are in equilibrium. We now know that the EPR-silent form was not detected during turnover because it was spin coupled to the heme iron. Therefore, it would be predicted that at 4 K, due to slower spin−spin transitions, the form of $VA^{\bullet+}$ that is spin-coupled would be detected, and the total concentration of $VA^{\bullet+}$ should be the same as that observed under acid quenched conditions. It can also be predicted that the concentration of $VA^{\bullet+}$, even at 4 K, will not exceed the concentration of LiP. In accord, spin concentration analysis at 4 K showed that the concentration of $VA^{\bullet+}$ detected during turnover never exceeded the concentration of LiP and that it equaled ∼95% of LiP concentration (Figure 4). For comparison, the data from a previous study (Khindaria et al., 1996) were also plotted in the same figure. The axis for the data at 4 K has been scaled to allow for a direct comparison with those obtained by acid quenching. The concentration (as a percentage of LiP) of the two species, $VA^{\bullet+}$ under acid quenched conditions and $VA^{\bullet+}$ at 4 K, are near identical. We then asked whether these species, at room temperature and at 4 K, were the same.

We explored this possibility by investigating the EPR signal of an acid quenched reaction mixture at 4 K. The EPR signal of $VA^{\bullet+}$ obtained upon acid quenching and rapid freezing was identical to that shown in Figure 2 (data not shown). This was in agreement with the spin-coupling analysis that suggested that the proton hyperfine structure is not affected by the oxoferryl moiety. However, the EPR signal in this case could not be saturated within the power range used to saturate the signal shown in Figure 2 (Figure 3). The failure to saturate the signal confirmed our earlier hypothesis that upon acid quenching the enzyme was denatured and the radical then neither interacts with the protein nor is stabilized by it.

Finally, we wanted to investigate the decay of the $VA^{\bullet+}$ EPR signal at 4 K. Equimolar concentrations of LiP, VA, and H_2O_2 were frozen at different times after the initiation of the reaction. The concentration of $VA^{\bullet+}$ as a function of reaction time are plotted in Figure 5. The decay of the EPR signal was fit to a first-order decay equation with a decay constant of 1.76 s^{-1}. This value is strikingly close to the decay constant of 1.85 s^{-1} obtained by two other methods (Khindaria et al., 1995b, 1996). This also served to verify our earlier assumption that the EPR-silent form of $VA^{\bullet+}$ is in equilibrium with the EPR-active form during turnover.

Concluding Remarks. To briefly review, LiPI oxidizes VA to $VA^{\bullet+}$, the majority of which is not released into the bulk solution (Khindaria et al., 1995b). The decay constant of the fraction that is released into bulk solution is 700 times greater than the decay constant for the fraction that stays associated with LiP (Khindaria et al., 1995b). The fraction that remains associated with the enzyme consists of an EPR-active form and EPR silent-form. The EPR-active and EPR-silent forms are in dynamic equilibrium. The $VA^{\bullet+}$ associated with LiPII is involved in subsequent catalysis (Khindaria et al., 1996). All this prompted us to call the intermediate a catalytic complex of LiPII−$VA^{\bullet+}$. However, before this study, the evidence for the presence of this complex was indirect. For the interaction of LiPII and $VA^{\bullet+}$ to be formally termed as a catalytic complex, there were three conditions that had to be fulfilled; first, there had to be physical "bonding" or "strong interaction" between the two species; second, there should be magnetic and electronic interaction between the two; and finally, individually the properties, spectral and catalytic, of the two had to be markedly different than as a complex. Therefore, there was need to unequivocally establish the properties of this complex.

The results compiled in this manuscript reveal some of the intricacies involved in the interaction of VA and LiP. This study attempted to understand the nature of interaction between LiPII and $VA^{\bullet+}$ and the properties of the LiPII−$VA^{\bullet+}$ complex. There were many phenomena involving $VA^{\bullet+}$ that were unexplained or had become conjectures based

on limited indirect evidence. For example, $VA^{\bullet+}$ accelerated the rate of reaction of LiPII with VA (Khindaria et al., 1995b). However, there was no known precedence to suggest that $VA^{\bullet+}$ could modulate the chemical and physical properties of LiPII or vice versa. However, we have shown that the $VA^{\bullet+}$ could be stabilized by LiP possibly due to the interaction of the radical with the protein or may have involved interaction with the heme (Khindaria et al., 1996).

The data presented resolve these speculations. Simulation of the 4 K EPR spectrum of $VA^{\bullet+}$ was possible only when the model took into account the interaction of the $S = 1$, oxoferryl moiety, with the $S = 1/2$ species, $VA^{\bullet+}$. Additionally, the fact that the EPR signal of $VA^{\bullet+}$ was relatively easily saturable suggested strong magnetic interaction between the two species. The magnetic interaction may be due to through-space or through-bond interaction. We tend to favor the latter and suggest a $\pi-\pi$ interaction between $VA^{\bullet+}$ and the porphyrin. The nitrogens of the porphryin in turn have π-bonding interaction with the iron. Molecular dynamics studies on trajectories of $VA^{\bullet+}$ (Khindaria & Aust, 1996) support this mechanism for the interaction. The angle of approximately 62° with the plane of the heme makes for strong $\pi-\pi$ interaction between the two. Additionally, this study served to verify the parameters that were previously deduced from indirect evidence (Khindaria et al., 1995a,b).

REFERENCES

Chung, N., & Aust, S. D. (1995) *Arch. Biochem. Biophys. 322*, 143−148.

Gilardi, C., Harvey, P. J., Cass, A. E. G., & Palmer, J. M. (1990) *Biochim. Biophys. Acta 1041*, 129−132.

Goodwin, D. C., Aust, S. D., & Grover, T. A. (1995) *Biochemistry 34*, 5060−5065.

Hammel, K. E., & Moen, M. A. (1991) *Enzyme Microbiol. Technol. 13*, 15−18.

Harvey, P. J., Schoemaker, H. E., & Palmer, J. M. (1986) *FEBS Lett. 195*, 242−246.

Hoffman, B. M., Roberts, J. E., Kang, C. H., & Margoliash, E. (1981) *J. Biol. Chem. 256*, 6556−6564.

Khindaria, A., & Aust, S. D. (1996) *Biochemistry 35*, 13107−13111.

Khindaria, A., Grover, T. A., & Aust, S. D. (1995a) *Biochemistry 34*, 6020−6025.

Khindaria, A., Yamazaki, I., & Aust, S. D. (1995b) *Biochemistry 34*, 16860−16869.

Khindaria, A., Yamazaki, I., & Aust, S. D. (1996) *Biochemistry 35*, 6418−6424.

Lundquist, K., & Kirk, T. K. (1978) *Phytochemistry 17*, 1676.

Poulos, T. P., Edwards, S. L., Wariishi, H., & Gold, M. H. (1993) *J. Biol. Chem. 268*, 4429−4440.

Rutter, R., Hager, L. P., Dhonau, H., Hendrich, M, Valentine, M., & Debrunner, P. (1984) *Biochemistry 23*, 6809−6816.

Sarkanen, K. V., & Ludvig, C. H. (1971) in Lignin: Occurrence, Formation and Structure, pp 1−18, Wiley-Interscience, New York.

Schultz, C. E., Devaney, P. W., Winkler, H., Debrunner, P. G., Doan, N., Chiang, R., Rutter, R. R., & Hager, L. P. (1979) *FEBS Lett. 103*, 102−105.

Shimada, M., Nakatsubo, F., Kirk, T. K., & Higuchi, T. (1981) *Arch. Microbiol. 129*, 321−324.

Tien, M., & Kirk, T. K. (1983) *Science 221*, 661−663.

Tien, M., & Kirk, T. K. (1984) *Proc. Natl. Acad. Sci. U.S.A. 81*, 2280−2284.

Tien, M., Kirk, T. K., Bull, C., & Fee, J. A. (1986) *J. Biol. Chem. 261*, 1687−1693.

Tuisel, H., Sinclair, R., Bumpus, J. A., Ashbaugh, W., Brock, B. J., & Aust, S. D. (1990) *Arch. Biochem. Biophys. 279*, 158−166.

BI9715730